A FEM DEFORMABLE MESH FOR ACTIVE REGION SEGMENTATION

Karteek Popuri, Dana Cobzas, Martin Jägersand

Computing Science,
University of Alberta, Canada

ABSTRACT

We propose a novel template-based multi-region segmentation method using a finite element method (FEM) deformation model with diffusion-based regularization. Our proposed method is computationally more efficient than the traditional template-based segmentation methods that use non-parametric or B-spline based deformation models, as it significantly reduces the number of degrees of freedom (DOF) associated with the energy minimization that arises in template-based segmentation. Further, like all template-based segmentation approaches our method is able to preserve topology of the initial regions of interest (ROIs) defined in the template, which is very useful for segmentation of anatomical structures. Segmentation results on medical images with various anatomical structures show that the proposed method improves computational efficiency without compromising segmentation accuracy.

Index Terms— Template-based segmentation, FEM model

1. INTRODUCTION

The segmentation of anatomical structures is a fundamental and challenging problem in medical image analysis. It often involves the simultaneous segmentation of multiple non-overlapping anatomical regions with weak boundaries. To further complicate matters the anatomical regions might share common boundaries. Over the years, the popular trend in medical image segmentation has been to use region-based energies within a level set based optimization framework [1]. But, the most desired feature of level sets, which is their ability to freely allow to for topological changes is actually a disadvantage in the case of medical images where the topology of the anatomical regions of interest (ROIs) is already known and needs to be maintained throughout the segmentation process. Besides, it is not trivial to extend the level set framework for multi-region segmentation (which is often required in medical images), as the evolving level sets corresponding to different regions might overlap with each other. Although, there exist level set based multi-region segmentation methods that solve this overlap problem, they still cannot prevent the undesired topology changes [2], [3]. Shape prior methods can be used to impose strict topological constraints on the evolving level set but they only assume a single ROI [4]. Recently, Fan *et al.* designed a multi-region homeomorphic segmentation approach by imposing topological constraints on a compact representation of the level set function [5].

Alternatively, we consider the template-based approach for topology preserving multi-region segmentation. In this approach, a template which is a label image defining the topology of the ROIs is smoothly deformed in a non-rigid registration framework such that a region-based energy is minimized to match the actual ROIs in the input image. The desired segmentation boundaries are then implicitly given by the contours of the initial ROIs defined in the template and the deformation field estimated between the template and the input image. Existing methods for template-based segmentation represent the deformation field using either a non-parametric deformation model [6] or the popular cubic B-splines based free form deformation (FFD) model [7], [8]. Consequently, these methods are forced to use a uniform discretization of the problem domain, which is inefficient because the deformation field is computed with the same accuracy everywhere even though detailed deformations are only needed along the contours of the ROIs. To address this issue, we propose a finite element method (FEM) deformation model, which parametrizes the deformation field on a non-uniform mesh well adapted to the contours of the ROIs in the template. This leads to a more computationally efficient solution as it involves minimization over a far fewer number of degrees of freedom (DOF) compared to the non-parametric and FFD deformation models. Further, we show that the use of a FEM model on a non-uniform mesh allows us to define the region-based energy directly on the input image domain. This is in contrast to the FFD model based methods [7], [8] that instead formulate the region-based energy on the template domain using the deformed input image, resulting in a "more non-convex" region-based energy which is undesirable. Another salient aspect of our FEM model is that the deformation field is explicitly regularized by solving the diffusion equation using the Galerkin FEM method. Shen *et al.* also used the FEM mesh in a segmentation framework but their method is only designed for a single object that is disambiguated from the background [9]. An older FEM edge-based segmentation method was proposed by Ferrant *et al.* but no region terms were defined in their case and therefore it would only work for objects with sharp boundaries [10].

To summarize, we make the following contributions:

(1) An efficient FEM-based solution to the template-based multi-region segmentation problem is presented.
(2) We designed a non-uniform FEM mesh with adaptive resolution on the template in order to obtain a low DOF parametrization of the deformation field.
(3) We are able to formulate the region-based energy on the original input image and estimate optimal deformations through iterative minimization with diffusion-based smoothing using the Galerkin FEM method.
(4) Validation on medical images containing various anatomical structures shows that the FEM deformation model obtains similar or better segmentation accuracies while using significantly lesser number of DOFs when compared to the existing works on template-based segmentation.

2. THEORY

2.1. FEM deformation model

We formulate the segmentation problem as the task of estimating a dense deformation field $\mathbf{U} : \Omega_T \rightarrow \Omega$ that defines optimal smooth

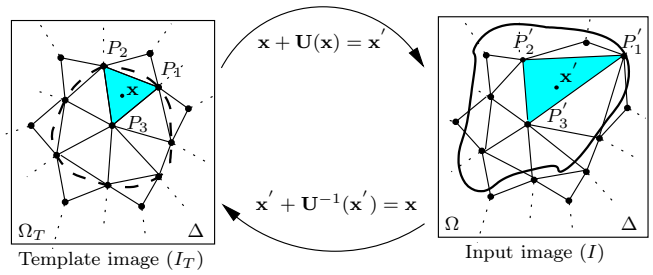

Fig. 1: Illustration of the deformable FEM mesh. The dashed closed curve in the template image (I_T) represents the boundary of the region of interest. The solid closed curve in the input image I represents the actual object boundary.

deformations of a template $I_T : \Omega_T \rightarrow \{1, 2, \ldots, R\}$ onto the image space $I : \Omega \rightarrow \mathbb{R}$ such that a region-based segmentation energy (defined in the next section) is minimized. Following the FEM formulation [11] , we approximate the deformation field as a linear combination of a set of piecewise-linear nodal basis functions (*hat* functions) $\{\phi_n\}_{n=1}^N$:

$$\mathbf{U}(\mathbf{x}) \approx \sum_{n=1}^{N} \mathbf{U}_n \phi_n(\mathbf{x}; \mathcal{M}) \quad \forall\, \mathbf{x} \in \Omega_T \tag{1}$$

The hat functions basis is defined on a discrete tesselation $\mathcal{M} = (\{P_n\}_{n=1}^N, \Delta)$ of the template domain Ω_T, where$\{P_n\}_{n=1}^N$ denotes the nodes of the mesh and Δ is the set of simplexes (triangles in 2D, tetrahedra in 3D) (see Figure 1).

Typically, in FFD deformation model based methods [7], [8] the energy is defined on the template domain Ω_T using the deformed input image $I(\mathbf{U}(\mathbf{x}))$ induced by the warp $\mathbf{U}$: $\mathbf{x}' = \mathbf{x} + \mathbf{U}(\mathbf{x})$. However, as mentioned earlier this makes the energy "more non-convex". Therefore, we define the region-based segmentation energy on the input image domain Ω by warping the template regions I_T with an inverse warp defined by $\mathbf{U}^{-1} : \mathbf{x} = \mathbf{x}' + \mathbf{U}^{-1}(\mathbf{x}')$ (see Eq. (4)). Similar to the above, we can approximate $\mathbf{U}^{-1}(\mathbf{x})$ on the deformed FEM mesh $\mathcal{M}' = (\{P_n'\}_{n=1}^N, \Delta)$ as:

$$\mathbf{U}^{-1}(\mathbf{x}') \approx \sum_{n=1}^{N} \mathbf{U}_n^{-1} \phi_n(\mathbf{x}'; \mathcal{M}') \quad \forall\, \mathbf{x}' \in \Omega \tag{2}$$

where $\mathbf{U}_n^{-1} \equiv \mathbf{U}^{-1}(P_n')$ is the value of the inverse deformation field at the node P_n'. It is easy to show that $\mathbf{U}_n^{-1} = -\mathbf{U}_n$, meaning that the value of the inverse deformation field at the nodal points of the deformed mesh $\mathcal{M}'$ is the *negative* of the deformation field at the nodal points of the original mesh $\mathcal{M}$. Thus, we can now re-write Eq. 2 as:

$$\mathbf{U}^{-1}(\mathbf{x}') \approx -\sum_{n=1}^{N} \mathbf{U}_n \phi_n(\mathbf{x}'; \mathcal{M}') \tag{3}$$

2.2. Multi-region segmentation using FEM deform. model

We now show how the FEM deformable model is used in the context of segmentation. Similar to a demons-like registration method [12], we decouple the data and regularization terms of an active region segmentation [13] model. We define the segmentation energy associated with the data term as:

$$E_D[\mathbf{U}] = -\sum_{r=1}^{R} \int_{\Omega} I_{Tr}(\mathbf{x}' + \mathbf{U}^{-1}) \log(p_r(I(\mathbf{x}'))) \, d\mathbf{x}' \tag{4}$$

where $\mathbf{U}^{-1} \equiv \mathbf{U}^{-1}(\mathbf{x}')$, the probability density $p_r(I(\mathbf{x}'))$ defines the intensity statistics for region r in Ω and $I_{Tr} : \Omega_T \rightarrow \{0, 1\}$ is a binary "region template" corresponding to each of the separate regions $r \in \{1, 2, \ldots, R\}$ defined in the template image I_T. For regularizing the deformation field we solve a diffusion equation: $\frac{\partial \mathbf{U}}{\partial t} = \mathrm{div}(\nabla \mathbf{U})$. Both the energy minimization and the diffusion equations are solved using the FEM framework. Incorporating the FEM model (see Section 2.1) into the multi-region segmentation energy (4) we obtain:

$$E_D(\{\mathbf{U}_n\}_{n=1}^N) = -\sum_{r=1}^{R} \int_{\Omega} I_{Tr}(\mathbf{x}' - \sum_{n=1}^{N} \mathbf{U}_n \phi_n(\mathbf{x}'; \mathcal{M}')) \log(p_r(I(\mathbf{x}'))) \, d\mathbf{x}' \tag{5}$$

To compute the set of nodal deformation field values $\{\mathbf{U}_n\}_{n=1}^N$ that minimize the above energy, we use a gradient descent approach where the gradient is defined by:

$$\frac{\partial E_D}{\partial \mathbf{U}_n} = \sum_{r=1}^{R} \int_{\Omega} w_n(\mathbf{x}') \nabla I_{Tr} \log(p_r(I(\mathbf{x}'))) \, d\mathbf{x}', \tag{6}$$

where $\nabla I_{Tr} \equiv \nabla I_{Tr}(\mathbf{x}' - \sum_{m=1}^{N} \mathbf{U}_m \phi_m(\mathbf{x}'; \mathcal{M}'))$ and $w_n(\mathbf{x}') = \sum_{m=1}^{N} \frac{\partial \phi_m(\mathbf{x}'; \mathcal{M}')}{\partial \mathbf{U}_n} \mathbf{U}_m + \phi_n(\mathbf{x}'; \mathcal{M}')$.

2.3. Demons-like approach for energy minimization

Following a demons-type framework [12], we iteratively solve for the final nodal deformation field $\mathbf{U}_n$ by composing the current estimates of the nodal deformation field $\mathbf{U}_n^k$ with a small nodal update field $\mathbf{u}_n^k$, i.e, $\mathbf{U}_n^{k+1} = \mathbf{U}_n^k \circ \mathbf{u}_n^k$. Further, at each step the nodal deformation field is smoothed using diffusion-like regularization. Nodal updates are computed based on the gradient of the energy (6):

$$\mathbf{u}_n^k = -\epsilon \sum_{r=1}^{R} \frac{\int_{\Omega} w_n^k(\mathbf{x}') \nabla I_{Tr}^k \log(p_r^k(I(\mathbf{x}'))) \, d\mathbf{x}'}{\int_{\Omega} w_n^k(\mathbf{x}') d\mathbf{x}'} \tag{7}$$

where ϵ is a small step size. The value of the update field $\mathbf{u}_n^k$ at a node P_n of the original mesh $\mathcal{M}$ can be interpreted as the negative of the weighted average of the region forces $\nabla I_{Tr}^k \log(p_r^k(I(\mathbf{x}')))$ at the pixels in the input image I that neighbor the corresponding node $(P_n')^k$ of the deformed mesh $(\mathcal{M}')^k$. The set of weights given by $\{w_n^k(\mathbf{x}')\}_{n=1}^N$ are independent of the information in the input image I and only depend on the deformed mesh $(\mathcal{M}')^k$ characteristics (the nodal basis functions $\{(\phi_n(\mathbf{x}'; \mathcal{M}'))^k\}_{n=1}^N$) and the estimate of the nodal deformation field $\mathbf{U}_n^k$.

Note that the weighted averaging implicitly acts as a viscous fluid-like regularization and thus our method does not require the expensive separate step for smoothing the update field. But we do need the diffusion-based regularization of the nodal deformation field $\mathbf{U}_n^{k+1}$ at each iteration that is performed by solving the diffusion equation $\frac{\partial \mathbf{U}}{\partial t} = \mathrm{div}(\nabla \mathbf{U})$. Following the Galerkin's FEM

Algorithm 1 FEM deform. model based multi-region segmentation

Input: I, I_T, $\mathcal{M}(\{P_n\}_{n=1}^N, \Delta)$
Output: $\mathbf{U}(P_n)$

1: At iteration $k = 0$, initialize $\mathbf{U}_n^0$
2: **while** $k <=$ max_iter and convergence not reached **do**
3: Compute region forces $\nabla I_{T_r}^k \log(p_r^k(I(\mathbf{x}^{'})) \; \forall$ pixels $\mathbf{x}^{'} \in \Omega$
4: Compute the weights $w_n^k(\mathbf{x}^{'}) \; \forall$ pixels $\mathbf{x}^{'} \in \Omega$
5: Compute the nodal updates according to Eq. 7
6: Update $\mathbf{U}_n^{k+1} = \mathbf{U}_n^k \circ \mathbf{u}_n^k$
7: Smooth deformation field $\mathbf{U}_n^{k+1}$ by solving a diffusion equation on a non-uniform mesh via FEM framework (see Eq. 9)
8: **end while**

framework, we consider the integral form of the diffusion equation:

$$E_S[\mathbf{U}^*] = \frac{1}{2}\int_\Omega \left[(\mathbf{U}^* - \mathbf{U})^2 + \alpha(|\nabla \mathbf{U}^*|^2)\right] d\mathbf{x} \qquad (8)$$

where $\mathbf{U}^*$ is the regularized deformation field we wish to estimate using the initial non-smooth deformation field $\mathbf{U}$ and α is the diffusion time. By vanishing it's first variation at each node P_n and restricting the minimization to a finite dimensional subspace spanned by the nodal basis functions $\{\phi_n\}_{n=1}^N$, we obtain a set of N linear equations for $m \in \{1, 2, \ldots, N\}$ as [11]:

$$\sum_{n=1}^{N}\left[\int_\Omega [\phi_n\phi_m + \alpha\,\nabla\phi_n.\nabla\phi_m]\, d\mathbf{x}\right]\mathbf{U}_n^* = \mathbf{U}_n \int_\Omega \phi_n\phi_m\, d\mathbf{x} \quad (9)$$

where $\mathbf{U}_n^*$ is the smoothed nodal deformation field. The above system of linear equations is very sparse, and the nodal integrals $\int_\Omega \phi_n\phi_m$, $\int_\Omega \nabla\phi_n\nabla\phi_m$ can be precomputed as they are independent of the nodal deformations $\mathbf{U}_n$. This greatly improves the overall computational speed of our proposed method. We summarize our proposed FEM-based segmentation in Algorithm 1.

2.4. Generation of the non-uniform mesh

The generation of a non-uniform mesh that is well adapted to the contours of the ROIs defined in the template is important for a good performance of our FEM-based segmentation methodology. For this purpose, we implemented the image-adaptive mesh generation strategy proposed by Yang *et.al* [14]. The basic idea of this method is to place mesh nodes in the image domain so that their spatial density varies according to the local image features. In our case, we place more points near the boundaries of the regions defined in the template. The subsequent Delaunay triangulation and the refinement steps automatically ensure that the fine triangular elements are placed around the contours while the coarse elements are used elsewhere (see column 2, Figure 2).

3. EXPERIMENTS

In this section, we evaluate our proposed FEM deformation model based multi-region segmentation method on real 2D medical images containing various anatomical structures of interest. We performed two sets of experiments, corresponding to the binary and multi-region segmentation cases respectively. In the following experiments, the template images were obtained from available manual segmentations of the corresponding anatomical structures. Further, the region intensity statistics in the input image were modeled using the Parzen probability density.

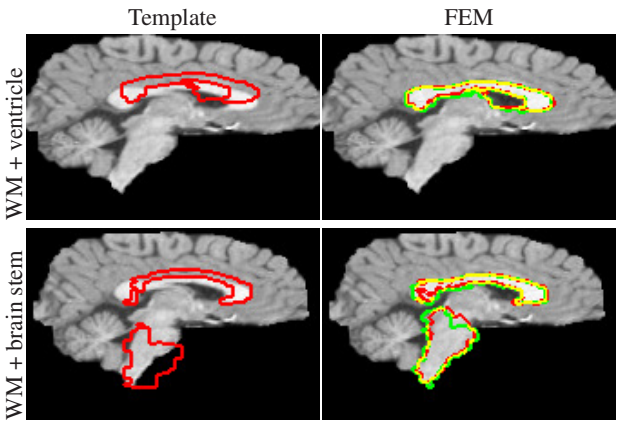

			Region 1	Region 2
	α	ϵ	Jaccard (%)	Jaccard (%)
WM (1) + Ventricle (2)	**1.0**	**2.0**	**79.51**	**73.53**
WM (1) + Brain stem (2)	**1.0**	**2.0**	**72.03**	**76.91**

Fig. 3: Multi-region segmentation results. Ground truth (green), estimated contours (red), overlap (yellow) - see colored figures.

3.1. Binary segmentation

We considered the segmentation of three different anatomical structures from 2D abdominal CT images namely the liver, spleen and muscle. We compared the results of our proposed FEM-based method with two other template-based segmentation methods which use the non-parametric [6] and FFD [8] deformation models respectively. All the template-based segmentation methods (including our proposed method) were implemented in a multi-resolution framework with three levels. The DOF corresponding to each of the template-based methods was computed as twice the sum of the number of nodes used in the mesh at each multi-resolution level. In Figure 2 we show the segmentation results obtained on the three different CT images using the three template-based segmentation methods. In addition we also show the results obtained using the classic level set based Chan-Vese segmentation method [1]. We initialized all the methods with the same template. Clearly, on all the three images our proposed method outperforms the Chan-Vese segmentation method. This is because our proposed method was successful in preserving the initial topology of the anatomical structures defined in the template. But, the simple region based Chan-Vese segmentation method "leaked" into neighboring structures with overlapping intensities disturbing the initial topology. More importantly, our proposed method achieves the highest computational efficiency among all the template-based methods as it uses a deformation model with a significantly lower ($\sim 1-2$ orders of magnitude) DOF compared to the FFD and non-parametric deformation models. Further, our method also obtains the highest Jaccard scores among all the template-based methods, except on the "spleen" image, where it performs only slightly worse than the non-parametric model based method.

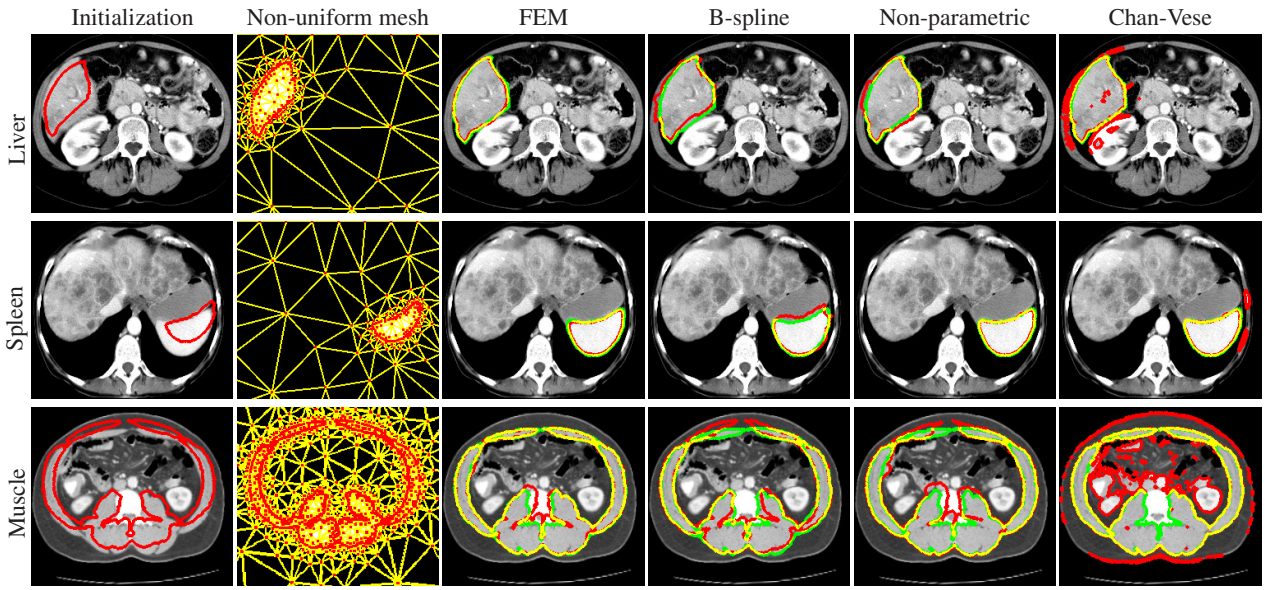

	FEM (proposed) non-uniform mesh				FFD [8] uniform mesh		Non-parametric [6] uniform mesh		Level set [1] Chan-Vese
	α	ϵ	DOF	Jaccard (%)	DOF	Jaccard (%)	DOF	Jaccard (%)	Jaccard (%)
Liver	**0.25**	**1.0**	**942**	**93.23**	43008	83.63	172032	89.07	83.65
Spleen	**0.25**	**1.0**	**774**	**89.95**	43008	80.80	172032	92.47	87.28
Muscle	**1.0**	**1.0**	**3310**	**85.92**	43008	74.60	172032	78.02	60.70

Fig. 2: Binary segmentation results. Ground truth (green), estimated contours (red), overlap (yellow) - see colored figures

3.2. Multi-region segmentation

We performed a combined segmentation of the cerebral white matter along with the ventricle and cerebral white matter along with the brain stem from 2D brain MRI images using our proposed method. The corresponding segmentation results and the Jaccard scores are shown in Figure 3. We see that the Cerbral white matter and the ventricle share a common boundary, whereas the brain stem has separate boundaries from the cerebral white matter. In both cases, our proposed method achieves good segmentation results.

4. CONCLUSIONS

We presented an efficient template-based segmentation framework which is particularly useful for the segmentation of anatomical structures that employs an adaptive non-uniform deformable FEM mesh.

5. REFERENCES

[1] D. Cremers, M. Rousson, and R. Deriche, "A review of statistical approaches to level set segmentation: integrating color, texture, motion and shape," *IJCV*, pp. 195–215, 2007.

[2] L. Vese and T.F. Chan, "A multiphase level set framework for image segmentation using the mumford and shah model," *IJCV*, vol. 50, pp. 271–293, 2002.

[3] T. Pock, A. Chambolle, H. Bischof, and D. Cremers, "A convex relaxation approach for computing minimal partitions," in *CVPR*, 2009.

[4] M. Rousson and N. Paragios, "Prior knowledge, level set representations & visual grouping," *International Journal of Computer Vision*, vol. 76, no. 3, pp. 231–243, 2008.

[5] Xian Fan, Pierre-Louis Bazin, John Bogovic, Ying Bai, and Jerry L. Prince, "A multiple geometric deformable model framework for homeomorphic 3d medical image segmentation," in *MMBIA at CVPR*, 2008.

[6] Kinda Anna Saddi, Christophe Chefd'hotel, Mikael Rousson, and Farida Cheriet, "Region-based segmentation via non-rigid template matching," in *MMBIA at ICCV*, 2007.

[7] X. Huang, D. Metaxas, and T. Chen, "Metamorphs: Deformable shape and texture models," in *Computer Vision and Pattern Recognition, 2004.* IEEE, 2004, vol. 1.

[8] C. Li and Y. Sun, "Active image: A shape and topology preserving segmentation method using b-spline free form deformations," in *ICIP*. IEEE, 2010, pp. 2221–2224.

[9] Tian Shen, Hongsheng Li, Zhen Qian, and Xiaolei Huang, "Active volume models for 3d medical image segmentation," in *CVPR*, 2009.

[10] Matthieu Ferrant, Olivier Cuisenaire, and Benoit Macq, "Multi-object segmentation of brain structures in 3d mri using a computerized atlas," in *SPIE Medical Imaging*, 1999.

[11] J.N. Reddy, *An introduction to the finite element method*, vol. 2, McGraw-Hill New York, 1993.

[12] T. Vercauteren, X. Pennec, A. Perchant, and N. Ayache, "Non-parametric diffeomorphic image registration with the demons algorithm," in *MICCAI*. Springer-Verlag, 2007, pp. 319–326.

[13] S.C. Zhu and A. Yuille, "Region competition: Unifying snakes, region growing, and Bayes/MDL for multiband image segmentation," *TPAMI*, vol. 18, no. 9, pp. 884–900, 2002.

[14] Y. Yang, N.M. Wernick, and G. Brankov, "A fast approach for accurate context-adaptive mesh generation," *IEEE transactions on image processing*, vol. 12, no. 8, pp. 866–881, 2003.